Acta Crystallographica Section D
Biological Crystallography
ISSN 0907-4449

The architecture of the GroEL–GroES–$(ADP)_7$ chaperonin complex. I. Heptagrammal molecular forms

A. Janner

Institute for Theoretical Physics, University of Nijmegen, Toernooiveld, 6525 ED Nijmegen, The Netherlands

Correspondence e-mail: alo@sci.kun.nl

Received 18 July 2002
Accepted 12 February 2003

Molecular forms are considered with vertices that have integral coordinates (the indices) with respect to a symmetry-adapted basis and which are left invariant by a point group of crystallographic scale-rotations (represented in this basis by invertible integral matrices). The composite form enclosing the chaperonin complex GroEL–GroES–$(ADP)_7$ is derived and decomposed into heptagrammal forms. These are generalizations of the two-dimensional forms based on sevenfold star polygons. In the chaperonin complex, nine such heptagrammal molecular forms are found: three for each ring (*trans* and *cis*) of GroEL and three for GroES. These forms correspond to a splitting of the monomer into adjacent segments. The change in the folding of the chains in the *cis* ring of GroEL arising from binding to GroES leaves the chain segmentation invariant.

1. Aim of the investigation

The sevenfold symmetry of the chaperonin GroEL and of its co-chaperonin GroES has been well known since the pioneering electron-microscopic investigation of Saibil & Wood (1993), who also showed that the double ring of the GroEL multimer is 'horizontally sliced', as pointed out by one of the referees.

The monomers of the two rings of GroEL and of GroES define an asymmetric unit of the point group of the complex, so that the folding of these monomers appears to be independent of any symmetry.

The aim of the present work is to show that this lack of symmetry is only apparent and is a consequence of the condition for the transformations to be Euclidean. It is taken for granted that for an Euclidean object, such as the geometrical structure of a molecule, only Euclidean transformations are meaningful and thus allowed. In fact, in addition to the sevenfold rotations, the molecular structure of GroEL–GroES also involves heptagrammal scalings. Therefore, the normal characterization above is incomplete because it does not consider crystallographic scale-rotations as possible transformations for molecules. In order to recognize the existence of this type of symmetry, a crystallography is required which includes point groups of infinite order (Janner, 2001*a*). This extension implies mathematical methods which are generally not familiar to crystallographers and to biochemists. In the present case, geometry helps one to grasp the new structural relations because the scale-rotations involved appear in a two-dimensional projection as star polygons that can be drawn by straight lines connecting the vertices of a regular polygon. In three dimensions, planes through these star polygons delimiting the molecule are considered. The situation then becomes analogous to that of crystal-growth forms obeying the Law of Rational Indices, which allows the

assignment of a set of rational integers to the crystal facets. In the biomacromolecular case, the rational indices are the coordinates of the vertices of the molecular form expressed with respect to a symmetry-adapted basis. It can then be recognized that the external envelopes are related to the central channels by invertible integral scaling transformations. In the GroEL–GroES complex, a similar scaling relation connects the envelope of GroEL to that of GroES. Moreover, the horizontal slicing mentioned above, normally associated with domains, appears to correspond to a decomposition of the molecular form of the whole into elementary forms, according to a partition of the monomers into adjacent segments. These elementary forms have symmetry properties that the domains after splitting do not possess. All this is presented here in part I.

2. Introduction

The GroEL chaperonin is a double-ring tetradecamer which assists protein folding. It binds to ATP molecules (or to ADP) and forms a complex with the heptameric co-chaperonin GroES (Branden & Tooze, 1999). The structures of the unliganded GroEL and GroES and of GroEL complexed with ATPγS and with GroES–$(ADP)_7$ have been determined in recent years (Boisvert *et al.*, 1996; Braig *et al.*, 1994; Hunt *et al.*, 1996; Xu *et al.*, 1997). The basic dynamic processes involved have also been elucidated (Lorimer, 1997; Rye *et al.*, 1997).

The sevenfold axial symmetry of both the unliganded and complexed structures is a characteristic feature and the question arises whether evidence for scalings compatible with the heptagonal symmetry can be found in these biomacromolecules. Within the frame of a general crystallography (Janner, 2001*a*), these are permitted crystallographic point-group transformations of infinite order. The same question has been positively answered in two other heptagonal cases: the nucleic acid poly-d(As^4T)·poly-d(As^4T) and the transmembrane pore protein α-haemolysin (Janner, 2002*a*). Compatible scaling transformations are not restricted to the cyclic point group of order seven and also occur in biomacromolecules with other axial symmetries. This has been shown for C-DNA and Z-DNA in hexagonal conformations (Janner, 2001*b*) and in the fivefold case of the human serum amyloid P component (Janner, 2002*b*). The easiest way to recognize geometrically the presence of point groups of infinite order is to look for polygrammal symmetries, which are scale-rotations that leave self-similar star polygons invariant. Their crystallographic nature appears arithmetically as groups of n-dimensional invertible integral matrices obtained by expressing the transformations with respect to a suitable basis.

The present investigation does not simply add new biomacromolecules to those indicated above, but is also intended to study the effect of an interaction which modifies the protein folding while keeping the scale-rotational point-group symmetry, as in the *cis* ring of GroEL when complexed with GroES (Xu *et al.*, 1997). It represents the very interesting case of different foldings of the same protomer: one in the unliganded state and one in the complexed state. The binding of ATP and of ADP, respectively, also modifies the structure of the chains, but this is a local effect involving more the biochemistry at a molecular-engineering level than the architecture itself of the protein, which in this paper represents the main concern.

The architecture of a building realises its functionality in terms of geometrical forms whose symmetries and proportions evoke harmony and style. In these terms, it could be said that the architecture of GroEL–GroES has the folding of other proteins as its functionality and is realised in a heptagonal polygrammal style with molecular forms having scale-rotation symmetries restricted by crystallographic laws. The crystallographic conditions enhance the harmonious interplay of the various forms and possibly the stability of the structure. The confinement of a given sequence of amino acids within the boundaries of a well defined molecular form normally requires folding of the chain at some given residues. As will be shown in part II (Janner, 2003*a*), these residues are mutually related by scale-rotation point-group elements, some of which also occur in the symmetry of the form.

This paper is based on structural data obtained from various PDB files reflecting different situations. Global considerations are required to allow a unifying point of view and the derivation of symmetry-adapted coordinates. This is performed in the next section. In §4 the molecular forms of GroEL are derived and in §5 those of GroES. These forms share scale-rotational symmetries, leading to an initial characterization of the chaperonin architecture as a whole. The last section concludes this first part and introduces the next paper, where some of the folding points of the tertiary structures, at the boundaries of the molecular forms, are related by scale-rotational point-group transformations. Mathematical aspects of the two- and three-dimensional point groups involved are outlined in an appendix. An initial analysis of the hidden order in GroEL–GroES–$(ADP)_7$ revealed by a molecular crystallography approach appears elsewhere (Janner, 2003*b*).

3. Symmetry-adapted coordinates

The investigation of scale-rotation symmetries in GroEL–GroES complexes is based on molecular crystallography, a possibility within a general crystallography, as explained in a previous paper (Janner, 2001*a*) and presented in a nutshell in Janner (2003*b*). The fundamental requirement of this crystallography is the existence of an n-dimensional faithful integral representation of the point group of the system considered. Lattice periodicity (clearly not realised in molecules which are aperiodic) leads to such representations, but is not required. In the molecular case (as for quasi-crystals) the integral representation is spanned by n vectors of the three-dimensional Euclidean space, which are linearly independent over the rationals and thus also over the rational integers $\mathbb{Z}$. By integral linear combinations, these vectors generate a $\mathbb{Z}$-module M of rank n, which is left invariant by the point group. The elements of the point group need not be Euclidean transformations and scalings are allowed, leading to point

groups of infinite order. The symmetry-adapted coordinates of the atomic positions are those expressed with respect to the basis of the $\mathbb{Z}$-module, in the same way as lattice coordinates are for the atoms of a crystal. For a given molecule, n basis vectors and the origin left invariant by the point group must be specified.

The smallest value of n for a heptagonal planar molecule is 6, which is the value of $\varphi(7)$, where φ is the number-theoretical Euler function. This follows from the requirement of linear independence over $\mathbb{Z}$. As GroEL and GroES are not planar, the minimal value for n is $\varphi(7) + 1 = 7$, with six vectors $a_1, a_2, \ldots, a_6$ in a plane pointing from the centre to the vertices of a regular heptagon and an additional non-coplanar vector a_7. A natural choice is a_7 along the sevenfold axis in the direction of the z axis and the other a_k in the xy plane of a Cartesian coordinate system. With respect to the orthonormal basis $e = \{e_1, e_2, e_3\}$, the symmetry-adapted basis adopted for GroEL–GroES is

$$a_k = a(\cos k\varphi, \sin k\varphi, 0), \quad \varphi = \frac{2\pi}{7}, k = 1, 2, \ldots, 6,$$
$$a_7 = c(0, 0, 1), \tag{1}$$

where

$$a_0 = -(a_1 + a_2 + \ldots + a_6) \tag{2}$$

is oriented along the x axis. The basis vectors $\{a_1, a_2, \ldots, a_7\}$ generate the $\mathbb{Z}$-module M and form the (a, c) basis. In order to verify the validity of this choice, the orientation of the various molecules has to be specified with respect to this basis, starting from the structural data found in the three PDB files: 1grl for the unliganded GroEL at 2.8 Å (Braig *et al.*, 1994), 1der for GroEL complexed with ATPγS at 2.4 Å (Boisvert *et al.*, 1996) and 1aon for the GroEL–GroES–$(ADP)_7$ complex at 3 Å (Xu *et al.*, 1997).

Disregarding local deviations, the *trans* rings of the unliganded GroEL, of GroEL–ATPγS and of GroEL–GroES–$(ADP)_7$ have the same structure. In the first two cases, the *cis* and *trans* rings are dyadically related and have the same molecular forms. Therefore, for GroEL, only two cases have to be considered: the *trans* ring, for example of GroEL–ATPγS, and the *cis* ring of GroEL–GroES–$(ADP)_7$.

For 1grl and 1der, the common origin is chosen at the intersection between the sevenfold axis and a dyad. This point was obtained by averaging the atomic positions of the residue Ala356 in the 14 chains of 1der and in the seven upper chains of 1grl. In the GroEL of 1aon there is no dyad relating the *trans* ring to the *cis* ring, a consequence of the interaction with GroES. However, the chains in the *trans* ring are only locally different from the corresponding chains in 1grl and in 1der, as has been pointed out previously (Boisvert *et al.*, 1996; Braig *et al.*, 1994). This property is exploited for orienting the 1aon data with respect to the two previous data sets by means of a translation (shifting the origin) followed by a rotation by an

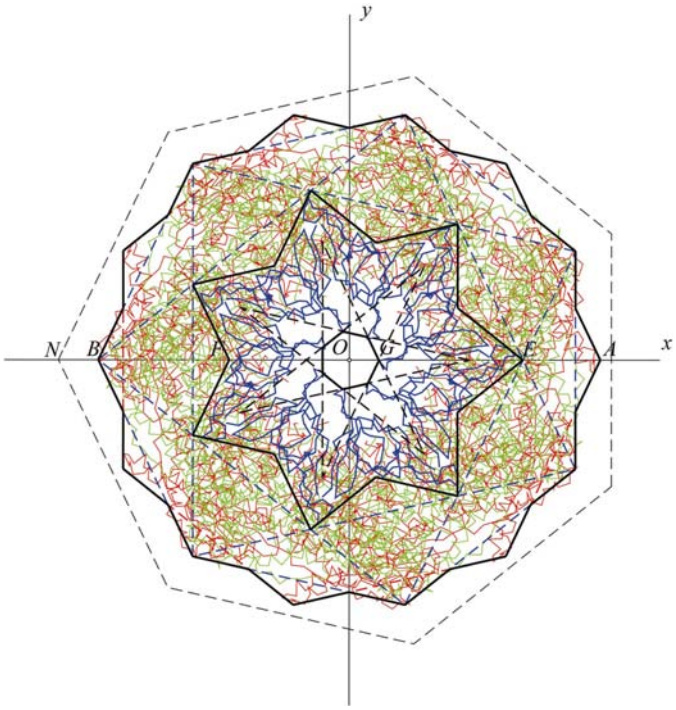

Figure 1
The heptagrammal symmetry of the GroEL–GroES chaperonin is demonstrated in a view along the sevenfold axis. The chains of GroES are drawn as thicker lines than those of GroEL.

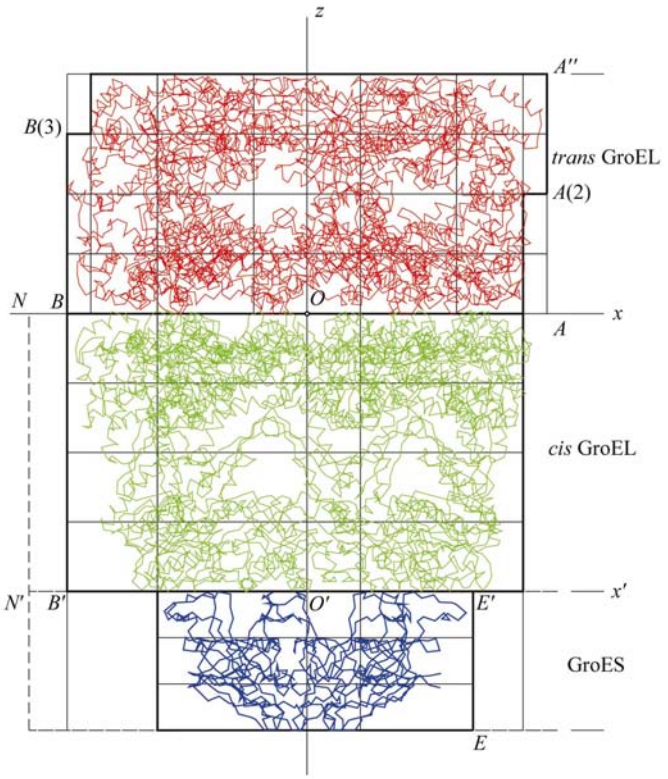

Figure 2
The *trans* ring and the *cis* ring of GroEL are shown in relation to GroES in a view perpendicular to the heptagonal axis. Small relative shifts along this axis allow the juxtaposed presentation. The thicker lines mark the prismatic boundaries of this global composite form, whereas the thinner horizontal lines correspond to planes which are $\mathbb{Z}$-module-equivalent to the bases of the various enveloping prisms. Note the metrical relations between the local $\mathbb{Z}$-modules: $OA = AA'' = OB$ for M_b, $ON = OO' = NN' = BB'$ for M_c and $EE' = \frac{1}{2}BB'$ for M_s.

angle γ around the z axis. The result is given here with lengths in ångströms.

$$\begin{aligned} 1\text{grl}: &\quad \text{translation} \quad (43.59, -1.55, 0.0) \\ &\quad \text{rotation} \quad \gamma = 0 \\ 1\text{der}: &\quad \text{translation} \quad (-83.61, -0.14, 26.7) \\ &\quad \text{rotation} \quad \gamma = \frac{\pi}{7} = 25.71^\circ \\ 1\text{aon}: &\quad \text{translation} \quad (-78.84, 51.59, -4.0) \\ &\quad \text{rotation} \quad \gamma = 11^\circ. \end{aligned} \tag{3}$$

These transformations also fix the positions of GroES, ATPγS and ADP molecules because they occur in one of the data sets indicated above. In the GroEL–GroES complex the *cis* ring is twisted by about 3° with respect to the *trans* ring, so that the value $\gamma = 8^\circ$ has been adopted for plotting the data of *trans* GroEL and of GroES (if nothing else is explicitly indicated), whereas for the GroEL–GroES complex as a whole the mean value $\gamma = 9.5^\circ$ has been adopted. The appropriate values for the structural parameters $a = |a_k|$, $k = 1, \ldots, 6$ and $c = |a_7|$ of the $\mathbb{Z}$-modules underlying the structure of the GroEL–GroES chaperonin complex follow from the prismatic heptagonal shape enclosing the biomacromolecules shown in Figs. 1 and 2 in two projections: along the sevenfold axis and perpendicular to it, respectively.

In Fig. 1 the heptagrammal scale-rotational symmetry of the GroEL–GroES complex is pointed out. The envelope of GroEL is formed by two regular heptagonal prisms. The vertex labelled A of the first prism is 70.3 Å from the centre O. The vertex labelled B is at the same axial distance and opposite A. It defines the second prism in x-reverse orientation. The envelope of GroES has vertices labelled E and F related to the envelope of GroEL by scale-rotations of the heptagrammal type {7/2}, as shown in Fig. 8 of the appendix. Starting from the vertex B of GroEL (in the reverse orientation with respect to Fig. 8), by constructing a {7/2} star heptagon (indicated by the dashed lines), the vertex E of the envelope of GroES is obtained. This implies that the radial distance OE is scaled with respect to OB by a factor $\mu_E = -1 + 2\cos\varphi - 2\cos 2\varphi = 0.6920\ldots$ The vertex F follows from E by another {7/2} star heptagon, which characterizes in axial projection the envelope of GroES.

The heptagrammal symmetry which connects the envelopes of GroEL and GroES also relate their channels. The central hole of GroEL [labelled by the vertex D shown in Fig. 5(*a*), but not here] follows from the A envelope by the {7/3} star-heptagon construction indicated in Fig. 8, so that the radial distance OD is scaled with respect to OA by a factor $\mu_D = -1 + 2\cos\varphi = 0.24697\ldots$ Finally, the central channel of GroES, with a vertex labelled G is also obtained by a {7/3} star heptagon (indicated in dashed lines) from a vertex opposite F. This implies that the radial distance OG is scaled with respect to OA by a factor $\mu_G = \mu_D\mu_E^2 = 0.11823\ldots$ (see Figs. 1 and 6).

These scaling relations are expressible in terms of invertible integral matrix transformations and ensure a common planar form of the $\mathbb{Z}$-modules, as discussed in the appendix.

The c parameters of the axial parts have a simple but hidden relationship to the a value. The first observation is that the height of the prism enveloping the *trans* ring of GroEL is equal to the radial heptagonal distance: $OA = OB = AA''$. The same is true for the *cis* ring but for the scaled distance $ON = NN' = \lambda_N OB$ with $\lambda_N = 4\cos\varphi + 6\cos 2\varphi = 1.1588\ldots$, a scaling factor leaving the planar $\mathbb{Z}$-module structure invariant, as shown in the appendix. Finally, the height of the enveloping prism of GroES is simply half that of *cis* GroEL: $EE' = \frac{1}{2}BB'$. In Fig. 2, *trans* GroEL, *cis* GroEL and GroES have been juxtaposed. This implies shifts along the z axis of 3.0 Å and ∼1.0 Å for the last two components, respectively, from the origin O defined by (3). Despite the existence of a common $\mathbb{Z}$-module for these shifted parts of the whole chaperonin, it is convenient to adopt the corresponding local $\mathbb{Z}$-modules M_t, M_c, M_s, respectively, for each component. The structural parameters of their basis are given by

$$\begin{aligned} \textit{trans}\ \text{GroEL}: &\quad M_t: \quad a_t = a, \quad c_t = a/4 \\ \textit{cis}\ \text{GroEL}: &\quad M_c: \quad a_c = a, \quad c_c = \lambda_N a/4 \\ \text{GroES}: &\quad M_s: \quad a_s = \mu_E a, \quad c_s = \lambda_N a/6, \end{aligned} \tag{4}$$

with $a = 70.3$ Å, $\lambda_N = 1.1588\ldots$ and $\mu_E = 0.6920\ldots$ The choice of the rational factors 1/4 and 1/6 is based on properties derived in the next two sections.

The heptagonal prisms enclosing the GroEL–GroES complex have vertices and faces with integral indices obtained by referring their coordinates to the basis of the corresponding $\mathbb{Z}$-module M_t, M_c or M_s. We recall that the common origin O is chosen at the intersection between the *trans* and the *cis* ring of GroEL. Some of these vertices have already been labelled. Their indices are given below as an example. Most of them can be read off from Figs. 1 and 2; the remainder follow from the information contained in the appendix. The following are found.

(i) For *trans* GroEL: using (1) with $a = c$, one obtains

$$(n_1\ n_2\ \ldots\ n_6, n_7)_t = \sum_{i=1}^{6} n_i a_i + \frac{n_7}{4} a_7. \tag{5}$$

Defining $A(n) = (\bar{1}\ \ldots\ \bar{1}, n)_t$ and $B(n) = (1\ \ldots\ 1, n)_t$ one obtains $A = A(0)$, $A'' = A(4)$ and $B = B(0)$.

(ii) For *cis* GroEL: $B = (1\ \ldots\ 1, 0)_c$, $B' = B(\bar{4}) = (1\ \ldots\ 1, \bar{4})_c$, where now

$$(n_1\ n_2\ \ldots\ n_6, n_7)_c = \sum_{i=1}^{6} n_i a_i + \frac{\lambda_N n_7}{4} a_7, \tag{6}$$

with $\lambda_N = 1.1588\ldots$

(iii) For the common channel of GroEL: in a similar way, $D(4) = (2\ 1\ 1\ 1\ 1\ 2, 4)_t$, $D = (2\ 1\ 1\ 1\ 1\ 2, 0)_c$, $D(\bar{4}) = (2\ 1\ 1\ 1\ 1\ 2, \bar{4})_c$.

(iv) For the external boundary of GroES: the indices are now defined with respect to the basis (a_s, c_s) of M_s,

$$(n_1\ n_2\ \ldots\ n_6, n_7)_s = \sum_{i=1}^{6} n_i \mu_E a_i + \frac{\lambda_N n_7}{6} a_7, \tag{7}$$

with $\mu_E = 0.6920\ldots$ and λ_N as above. One then obtains

$$E' = (2\ 0\ 1\ 1\ 0\ 2, \bar{4})_c = (\bar{1}\ \ldots\ \bar{1}, \bar{6})_s,$$
$$E = (\bar{1}\ \ldots\ \bar{1}, \bar{9})_s,$$
$$F' = (\bar{2}\ 0\ \bar{1}\ \bar{1}\ 0\ \bar{2}, \bar{6})_s,$$
$$F = (\bar{2}\ 0\ \bar{1}\ \bar{1}\ 0\ \bar{2}, \bar{9})_s. \quad (8)$$

(v) For the central hole of GroES:

$$G' = (\bar{6}\ \bar{1}\ \bar{4}\ \bar{4}\ \bar{1}\ \bar{6}, \bar{6})_s, \quad G = (\bar{6}\ \bar{1}\ \bar{4}\ \bar{4}\ \bar{1}\ \bar{6}, \bar{9})_s.$$

The global analysis given so far allows the decomposition of the quaternary structure of the GroEL–GroES complex into molecular forms in a way which reflects the decomposition in domains and in regions of the tertiary structures involved. However, domains and regions are not the same as molecular forms, because forms require invariance with respect to the point group of a given $\mathbb{Z}$-module, as discussed in a previous paper (Janner, 2001*a*). The derivation of the molecular forms of GroEL and GroES given in the following two sections is inductive and not deductive. These forms are first obtained as heptagonal prisms with integral indices enclosing chain segments. The point-group invariance of these forms is postponed to the appendix.

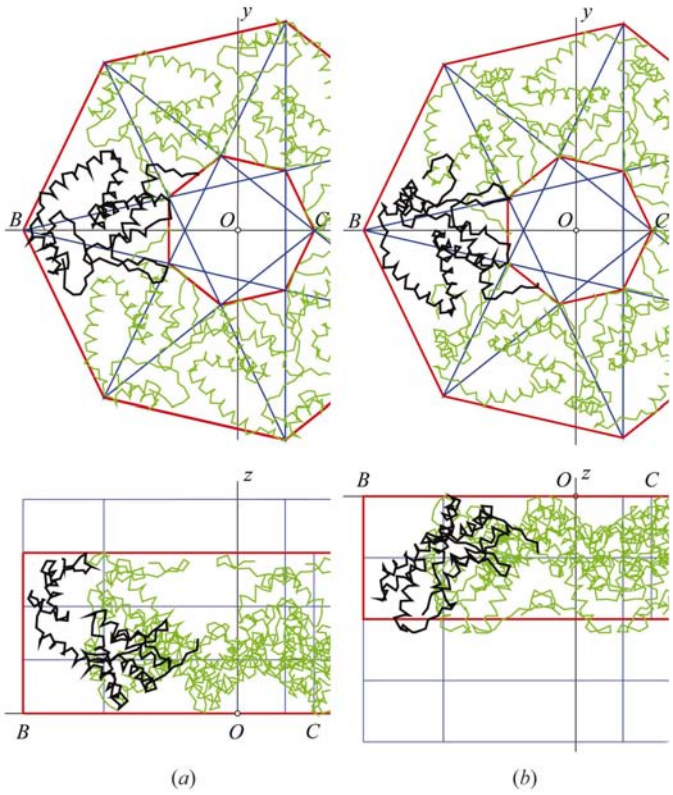

Figure 3
(*a*) N-terminal form of *trans* GroEL. It envelops the segments from Ala2 to Leu187 of the chains *H* to *N* (PDB code 1der; a = 70 Å, γ = 0). (*b*) N-terminal form of *cis* GroEL. As in the case of the *trans* ring, the segments of the chains *A* to *G* range from Ala2 to Leu187. The scaling relation between external boundary and central hole is also the same, but the folding is different (PDB code 1aon; a = 70.3 Å, $\gamma = 8°$)

4. GroEL molecular forms

As in the case of crystals, the word *form* has a technical meaning and it is not the same as *shape*. For crystals, a form consists of a set of point-group-equivalent lattice planes (Bürger, 1956) and for molecules it implies a set of point-group-equivalent $\mathbb{Z}$-module planes and vertices. The two requirements are not mutually exclusive, as can be learned from snow crystals (Janner, 2002*c*). The observed enclosing shape of GroEL–GroES is in fact composed of different forms.

From these symmetry requirements follows a *Law of Rational Indices* which implies that a set of n integers (the *indices*) can be assigned to the vertices of a molecular form. These indices are nothing other than the coordinates of the vertices expressed with respect to a basis (of rank n) of the $\mathbb{Z}$-module. If fractional indices instead of integers are found, this may mean that the basis adopted only generates a submodule. As for crystals, the indices of a delimiting plane are the coordinates of a vector normal to the face expressed with respect to the dual $\mathbb{Z}$-module (not discussed further here). A law of rational indices is only meaningful if there is the possibility of an experimental distinction between rational and irrational coordinates. This is the case for relatively small indices (or for reduced fractions of small integers) for forms enclosing the given set of atoms reasonably well. The criterion adopted here for 'small' is integers with an absolute value not much larger than ten. At the present level of experience, it is difficult to be more precise. The best one can do is to apply the general concepts to specific cases.

4.1. Forms of the *trans* ring of GroEL

Figs. 1 and 2 reveal two morphological properties of the *trans* ring of GroEL.

(i) *Trans* GroEL consists of at least two different molecular forms: one based on the regular heptagon (in the positive x orientation), labelled A, with vertices at a_k, $k = 1, \ldots, 6$, and the reverse one, labelled B (in the negative x orientation), with vertices at $-a_k$.

(ii) The height h_t of the *trans* ring is equal to the radius $r = |a_0| = 70.3$ Å, as already mentioned in the previous section for GroEL–GroES–$(ADP)_7$. In GroEL–$(ATP\gamma S)_{14}$, $|a_0| = 71$ Å is a better approximation.

In the uncomplexed state of GroEL, the two regular heptagons are in the only possible orientations allowed by the dyad axis, chosen here along the x axis. One way to arrive at the molecular forms of the *trans* ring is to consider the three domains discussed by Braig *et al.* (1994): (i) the equatorial domain, residues Val6–Ala133 and Glu409–Asp523, (ii) the intermediate domain, residues Leu134–Val190 and Ala377–Glu408, and (iii) the apical domain, residues Glu191–Val376.

All these domains have height $h_t/2$. The equatorial domain extends (approximately) from $z = 0$ to $z = h_t/2$, the intermediate domain from $z = h_t/4$ to $z = 3h_t/4$ and the apical domain from $z = h_t/2$ to $z = h_t$. One of the two heptagons considered above (labelled A and B, respectively) can be taken as a basis for the heptagonal prism enclosing a corresponding domain. The integral indexing of these prisms

requires a $\mathbb{Z}$-module with structural parameters a_t and c_t as chosen for M_t in (4). For the forms in question it is also necessary to consider the heptagonal prisms of the central holes. In order to allow integral indexing, the scale-rotation which transforms the heptagon of the external envelope into the one of the corresponding holes has to satisfy crystallographic conditions leading to integral invertible matrices. This is particularly the case for the polygrammal transformations of star heptagons, as shown in a previous paper (Janner, 2002*a*) and presented again in the appendix. In the present case, holes with good properties are indeed found, but the existence of two different central holes in the intermediate domain is then recognized: one (labelled *C*) delimited by residue Lys65 and scaled by $\mu_C = 2\cos\varphi + 4\cos 2\varphi = 0.3569\ldots$ with respect to *OA* and one (labelled *D*) delimited by residue Pro525 and scaled by $\mu_D = 0.2469\ldots$ as already considered in the previous section. Both scaling factors occur in the star heptagon {7/3}. Moreover, the two holes arise from disconnected segments of the protomer. These observations suggest the consideration of forms obtained from a given connected segment of the protomer and satisfying the restrictions imposed by the $\mathbb{Z}$-module M_t. The three forms represented in Figs. 3(*a*), 4(*a*) and 5(*a*) are then obtained. A first form (Fig. 3*a*) envelops the N-terminal segments of the seven chains *H* to *N* of 1der (or of 1aon), ranging from residues Ala2 to Leu187. The second form (Fig. 4*a*) corresponds to the apical domain and is given by the intermediate segments ranging from residues Leu187 to Val376. Finally, the third form (Fig. 5*a*) is obtained from the C-terminal segment and ranges from residues Val376 to Lys526 (or Pro525 in 1aon).

The validity of a heptagrammal scaling connecting the external prism to the internal one for these three forms is indicated graphically by a star heptagon in the view along the sevenfold axis of the corresponding figure and by heights at the regular intervals required by the $\mathbb{Z}$-module M_t in the alternative perpendicular view. The labels of some representative vertices are correspondingly the same as those given in Figs. 1 and 2 and those already indexed in the previous section. The planar indices of the point *C* (appearing in Figs. 3*a* and 4*a*) are (1 2 0 0 2 1) and the corresponding axial indices are 0, 2, 3 or 4 depending on the case considered. The indices of the faces of the prisms are so simple that no special explanation is required.

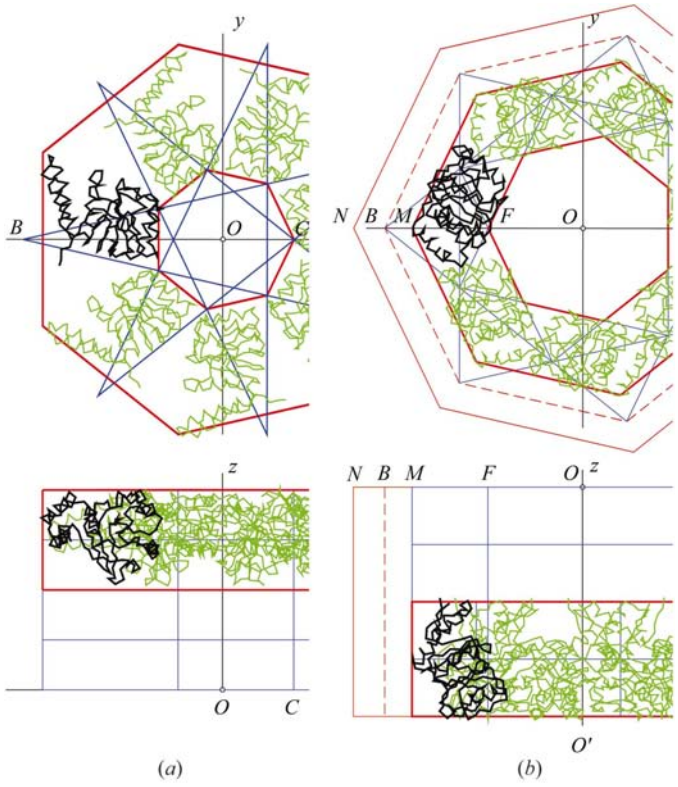

Figure 4
(*a*) Intermediate form of *trans* GroEL. The segments range from Leu187 to Val376 and correspond to the apical domain. The central hole is related to the external boundary by a inverted {7/3} star heptagon leading to a scaling factor $\mu_C = 0.3569\ldots$ (PDB code 1der). (*b*) Intermediate form of *cis* GroEL with segments of the chains *A* to *G* ranging from Leu187 to Val378, instead of Val376 as in the *trans*-ring case. The central hole is now based on a repeated {7/2} star-heptagon construction from the *B* heptagon which, however, no longer represents the lateral faces (PDB code 1aon). The two heptagons labelled *N* (see Figs. 1 and 2) and *M* are obtained from the *B* heptagon by the inverse scaling transformations S_{λ_N} and $S_{\mu_N} = S_{\lambda_N}^{-1}$, respectively.

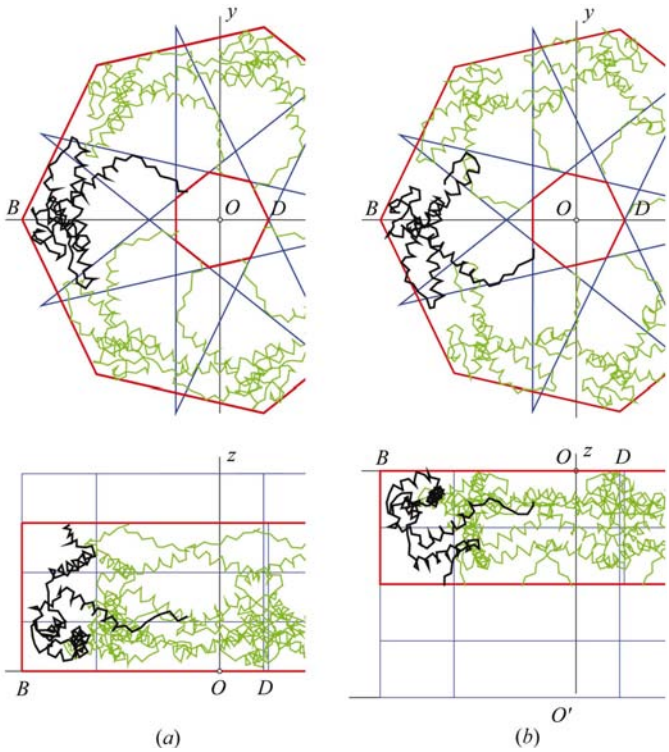

Figure 5
(*a*) C-terminal form of *trans* GroEL with segments from Val376 to Lys526. The central hole is related to the external boundary by a {7/3} star heptagon (as in Fig. 3), but now in an inverted orientation and with a scaling factor $-\mu_D = -0.2469\ldots$. (PDB code 1der). (*b*) C-terminal form of *cis* GroEL with segments ranging from Val378 to Pro525. In the axial projection this form looks the same as in the *trans* ring, but not in the perpendicular projection. This reflects the change in the folding (PDB code 1aon) arising from binding to GroES.

4.2. Forms of the *cis* ring of GroEL in GroEL–GroES–(ADP)$_7$

Without binding to GroES, the *cis* ring of GroEL is simply a dyadic image of the *trans* ring and therefore also of the corresponding molecular forms. The formation of a complex with GroES only marginally modifies the *trans* ring, as already mentioned, but has a profound influence on the *cis* ring, which binds GroES. In particular, the height of the *cis* ring is increased by a factor $\lambda_N = 1.1588\ldots$ and becomes twice the height of GroES. The axial submodule is changed accordingly, while keeping the same planar heptagonal submodule which is shared by GroES. It is therefore probably not an accident that λ_N is a scaling factor that leaves the heptagonal $\mathbb{Z}$-module invariant, as shown in the appendix.

These considerations suggest adopting the same splitting for the *cis* ring as for the *trans* ring. This approach appears to be the correct one, despite the fact that a somewhat better fitting is obtained if Val378 is taken instead of Val376 as the transition between the intermediate and the C-terminal forms. Three molecular forms are again obtained with point-group equivalent integral indices for the faces and the vertices. Because of the binding to GroES, these forms are similar to, but different from, those of the *trans* ring (see Figs. 3*b*, 4*b*, 5*b* and Table 1). The two N-terminal forms (in contact at the plane $z = 0$) have correspondingly the same external (B) and internal (C) heptagons (see Figs. 3*a* and 3*b*). The heights are different and in the *cis*-ring case there are deviations from the ideal boundary required by the axial $\mathbb{Z}$-module. Most of the indices of the vertices labelled have the planar values already indicated above. A difference is the heptagon (labelled M) occurring in the intermediate form. It is scaled by a factor $1/\lambda_N = \mu_N = 2 - 4\cos\varphi + 2\cos 2\varphi - 2\cos 3\varphi = 0.86293\ldots$ from that labelled B (see Fig. 4*b*). The heptagon of the central hole at F is scaled with respect to the point B by a factor $\mu_E^2 = (0.692\ldots)^2$, so that the ratio between the external M heptagon and the internal one is $\mu_N^{-1}\mu_E^2 = 0.5549\ldots$ Accordingly, the indices of the corresponding vertices are

$$\begin{aligned} M' = M(-4) &= (4\ 1\ 3\ 3\ 1\ 4, \bar{4})_c, \\ M(-2) &= (4\ 1\ 3\ 3\ 1\ 4, \bar{2})_c, \\ F' = F(-4) &= (9\ 2\ 6\ 6\ 2\ 9, \bar{4})_c, \\ F(-2) &= (9\ 2\ 6\ 6\ 2\ 9, \bar{2})_c. \end{aligned} \tag{9}$$

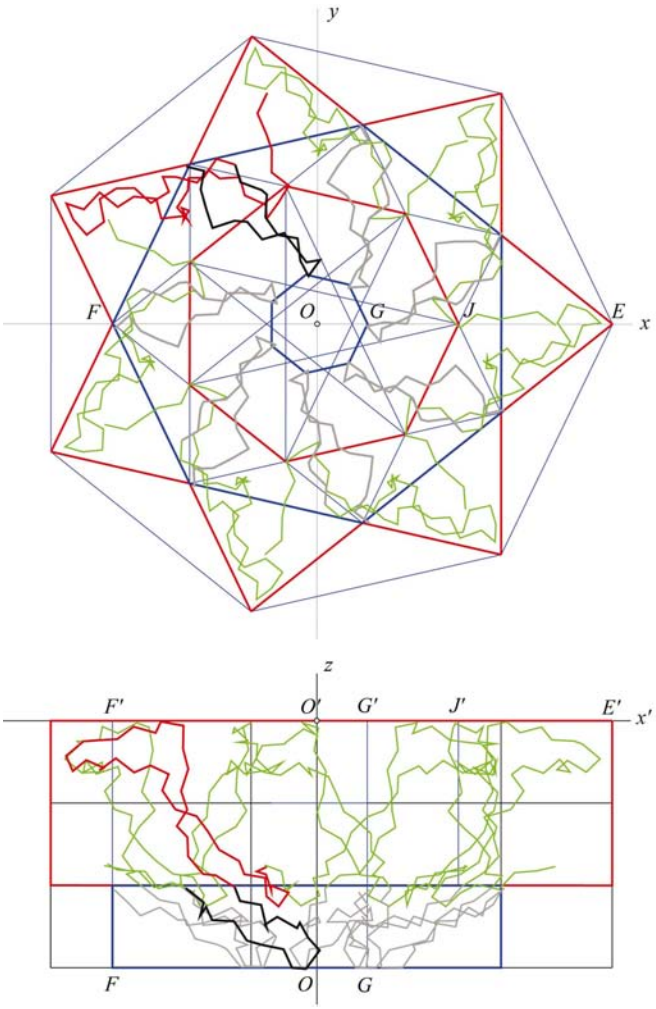

Figure 6
N-terminal form of the co-chaperonin GroES in the complexed state spanned by the segments of the seven chains *O* to *U* from Met1 to Ala42. In the axial projection, the external boundary corresponds to a {7/2} star heptagon. The central channel heptagon, labelled *J*, follows from the vertex *F* by a {7/2} star-heptagon construction. The intermediate form of GroES follows from the segments ranging from Ala42 to Gly62. It corresponds to what is called the 'roof' of GroES. The central hole is in an inverted {7/3} star-polygon relation with respect to the external heptagonal boundary.

Table 1
Comparison of the molecular forms of heptameric chain segments in the *trans* and the *cis* rings of GroEL.

By a dyadic transformation applied to the *trans* ring one obtains the forms of the *cis* ring in the uncomplexed state.

Form	Ring	Segments	Lateral confinement	Basal confinement	Scaling factor hole/ext. boundary	Fig.
N-terminal	*trans*	2–187	*B–C*	0–3	−0.35...	3(*a*)
	cis	2–187	*B–C*	0–$\bar{2}$	−0.35...	3(*b*)
Intermediate	*trans*	187–376	*A–C*	2–4	0.35...	4(*a*)
	cis	187–378	*M–F*	$\bar{2}$–$\bar{4}$	0.55...	4(*b*)
C-terminal	*trans*	376–525	*B–D*	0–3	−0.24...	5(*a*)
	cis	378–525	*B–D*	0–$\bar{2}$	−0.24...	5(*b*)

5. GroES molecular forms

The co-chaperonin GroES consists of seven subunits, each with nine β-strands. In the unliganded conformation there is a long mobile loop forming a β-hairpin ranging from residues Glu16 to Ala33. This segment is stabilized by GroEL and becomes a binding loop. Another segment with the residues from Pro56 to Phe67 forming the 'roof' of the dome-shaped GroES can also be distinguished (Hunt *et al.*, 1996; Xu *et al.*, 1997). No separate domains have been considered in this protein.

The perpendicular view of GroES given in Fig. 2 suggests a splitting of the protomer into segments leading to forms that

are a multiple of $\frac{1}{3}h_s$ high, where h_s is the height of GroES. This is indeed possible by splitting each monomer into three adjacent segments, in a similar way as for the GroEL rings.

The N-terminal segment of GroES ranges from Met1 to Ala42 and includes the binding loop (Lys15–Thr36). It is approximately $\frac{2}{3}h_s$ high and has a central heptagonal hole (labelled J) scaled by a factor $\mu_E^2 = (0.692\ldots)^2$ from the vertex E and by a factor $\mu_E = -0.692\ldots$ from the vertex F, respectively, of the external {7/2} star polygon (see Fig. 6). As already pointed out, these scaling relations fit those of the intermediate form of the *cis* ring of GroEL, at the interface where the complex binding occurs (see Fig. 4*b*). Indeed, starting from the vertex at $B(\bar{4})$ of the GroEL form, one obtains by successive {7/2} star-polygon constructions the vertices labelled $E(\bar{6})$, $F(\bar{6})$ and $J(\bar{6})$ of the adjacent GroES form. According to the convention adopted in (8), the indices of these coplanar vertices are given by

$$\begin{aligned} B(\bar{4}) &= (1\ 1\ 1\ 1\ 1\ 1, \bar{4})_c = (1\ 2\ 1\ 1\ 2\ 1, \bar{6})_s, \\ E(\bar{6}) &= (\bar{1}\ \bar{1}\ \bar{1}\ \bar{1}\ \bar{1}\ \bar{1}, \bar{6})_s, \\ F(\bar{6}) &= (\bar{2}\ 0\ \bar{1}\ \bar{1}\ 0\ \bar{2}, \bar{6})_s, \\ J(\bar{6}) &= (\bar{9}\ \bar{2}\ \bar{6}\ \bar{6}\ \bar{2}\ \bar{9}, \bar{6})_s \end{aligned} \tag{10}$$

and correspondingly lower vertices at $E(\bar{8})$, $F(\bar{8})$ and $J(\bar{8})$. The other vertices of the N-terminal form follow from the heptagonal rotational symmetry.

The intermediate form is obtained from the segments ranging from Ala42 to Gly62. It corresponds to what is called the 'roof' of GroES. The enclosing prism of this roof is $\frac{1}{3}h_s$ high and has bases confined by external heptagons at $F(\bar{8})$ and at $F(\bar{9})$ and by a central heptagonal hole at $G(\bar{8})$ and at $G(\bar{9})$. The hole is in a reverse {7/3} relation with the external boundary (see Fig. 6). This implies the scaling relation

$$G = S_{-\mu_D} F, \quad \mu_D = 0.24697\ldots \tag{11}$$

The labels adopted here are those appearing in Figs. 1 and 2. The corresponding indices have already been given.

The third form encloses the remaining C-terminal segments (Gly62–Ala97) of the seven chains O to U of 1aon, as shown in Fig. 7. The perpendicular view reveals that this form occupies the region ranging from 1/3 to 2/3 of the total height h_s. The central hole appears in the axial view as a regular heptagon (labelled I) scaled by a factor $-\mu_C = -0.3569\ldots$ with respect to the larger heptagon E of the N-terminal form. This means that it can be obtained from it by a {7/3} star-polygon construction, as indicated in Fig. 7. With respect to the B heptagon of GroEL it is scaled by a factor $\mu_C\mu_E = \mu_D = 0.2469\ldots$, whereas the external heptagon (labelled H) is scaled with respect to B by a factor $-\mu_H = 1 + 4\cos\varphi + 2\cos 2\varphi + 4\cos 3\varphi = -0.55495\ldots$. All these scaling transformations leave the heptagonal $\mathbb{Z}$-module M_s invariant. Summarizing, one obtains

$$\begin{aligned} OH &= -\mu_H OB \quad \text{with } \mu_H = 0.5549\ldots, \\ OI &= \mu_D OB \quad \text{with } \mu_D = 0.2469\ldots \end{aligned} \tag{12}$$

with indexed positions

$$H(\bar{8}) = (1\ 0\ 1\ 1\ 0\ 1, \bar{8})_s, \quad I(\bar{8}) = (\bar{1}\ \bar{2}\ 0\ 0\ \bar{2}\ \bar{1}, \bar{8})_s \tag{13}$$

and $H(\bar{7})$, $I(\bar{7})$ with correspondingly the same planar indices.

One can refine the prismatic form approximation taking other limiting planes into account. The determination of the indices of the faces then requires further information on the properties of the dual $\mathbb{Z}$-module M_s^* (in the case of GroEL also M_i^* and M_c^*). This goes beyond the aim of the present contribution.

6. Discussion

The present work demonstrates the existence of molecular forms obeying general crystallographic laws leading to vertices with integer indices. The analysis of this fundamental property in the particular case of the GroEL–GroES complex allows a number of further conclusions to be drawn.

The first conclusion that can be drawn from the indexed forms of GroEL and GroES is that both co-chaperonins share not only the sevenfold rotational symmetry but also the associated heptagrammal scalings. This ensures a great compatibility between GroEL and GroES despite the difference in size, as expressed by their alternative names CPN60

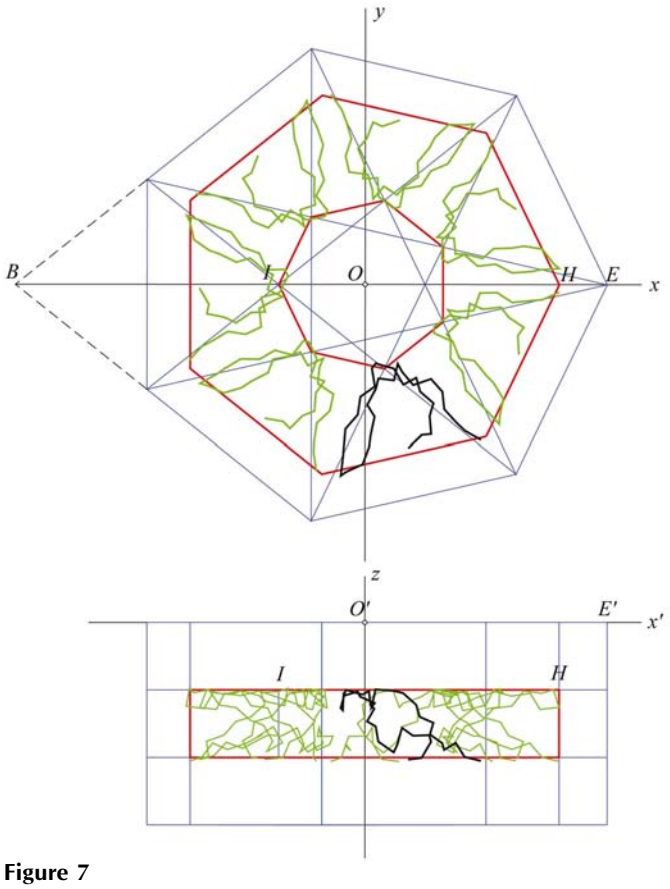

Figure 7
C-terminal form of GroES with segments ranging from Gly62 to Ala97. It corresponds to the central 1/3 slice of the prism enveloping GroES. The central hole follows by a {7/3} star-heptagon construction from the heptagon labelled E which, however, does not represent the external boundary. The situation is similar to the intermediate form of *cis* GroEL (Fig. 4*b*). In both cases the external boundary is still related to the hole by a scaling transformation that leaves the $\mathbb{Z}$-module invariant.

and CPN10. In particular, the vertices of the two forms at the GroEL–GroES binding interface have integral indices with respect to a common symmetry-adapted basis.

The second conclusion is that the deformation of the *cis* ring of GroEL induced by the binding with GroES is such that it extends the planar compatibility pointed out above to the axial direction. This is already apparent from the relation in heights $h_c = 2h_s$, where h_c and h_s are the heights of the GroEL *cis* ring and of GroES, respectively. Moreover, the forms of the *cis* ring are modified in such a way that their vertices also have integral axial coordinates in the symmetry-adapted basis of GroES. One obtains the correspondence

$$n_{7c} = 0, \bar{2}, \bar{4} \longleftrightarrow n_{7s} = 0, \bar{3}, \bar{6}.$$

The third conclusion is that the segmentation of the chains of GroEL, giving rise to the various enveloping forms, is conserved under the polymorphic transformation induced by the binding with GroES. This is indicated in Table 1, together with other relations summarized without further comment.

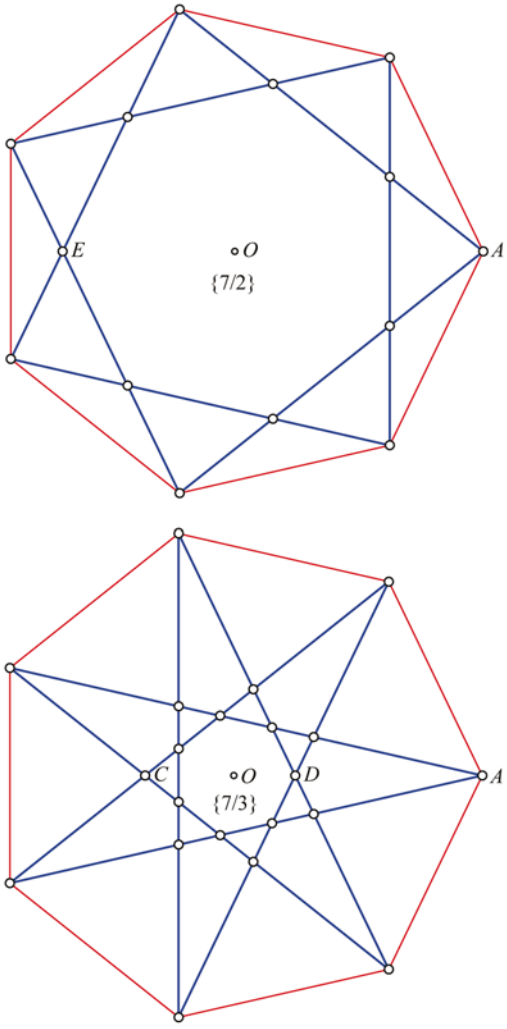

Figure 8
The star heptagons {7/2} and {7/3} with vertices labelled as in the various forms of GroEL–GroES (up to a possible inversion).

Finally, a last remark. A chaperonin mediates the folding of other proteins. The folding of the chaperonin itself is certainly relevant to understanding this function. The present work does not pretend to solve the problem, not even in part II where folding enters explicitly into the picture (Janner, 2003*a*). As in the case of crystals, the study of enclosing forms represents a first stage which allows the recognition of the existence of structural relations justifying at the atomic level the geometry of the form. In the second part, folding points are analyzed which are implied by the regular forms delimiting the volume occupied by parts of the GroEL–GroES complex. The positions occupied by the ATP and ADT molecules in these forms will also be considered.

APPENDIX *A*

A1. Heptagrammal molecular forms

Given is a $\mathbb{Z}$-module $M = \langle a_1, \ldots, a_7 \rangle$ of rank 7, whose elements are the integral linear combinations of the vectors

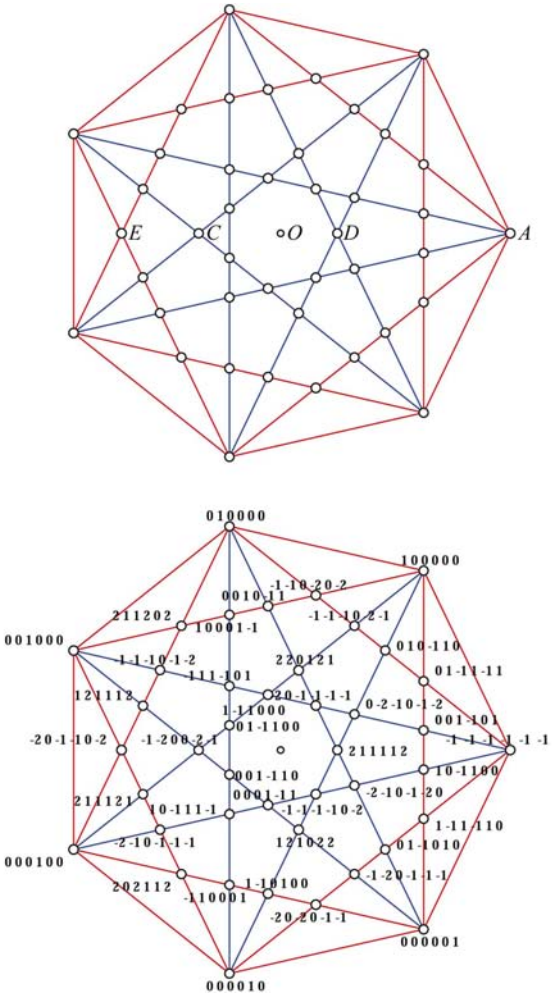

Figure 9
The planar heptagram obtained from a combination of a regular heptagon and the two star heptagons of Fig. 8. The intersection points have the integral indices indicated and correspond to elements of the heptagonal $\mathbb{Z}$-module, which in the planar case is of rank six.

$a_1, a_2, \ldots, a_7$ defined as in (1) and forming the basis (a, c) of M,

$$M \ni m = (n_1 \ldots n_6, n_7) = \sum_{i=1}^{7} n_i a_i, \quad n_i \in \mathbb{Z} \tag{15}$$

with $n_1, \ldots, n_7$ the *indices* of the vector m.

An M-invariant *molecular form* is defined in three-dimensional affine space (it is simply called a form). This implies that the vertices of the form have *rational indices*. This means that after the choice of the origin and with respect to the basis (a, c) the vertices have integral coordinates.

A *heptagrammal form* is an M-invariant form with heptagonal symmetry. The point group K of the form is generated by linear transformations T leaving the set of vertices and the $\mathbb{Z}$-module M invariant. It means that there is a pair of vertices U, V transformed into another by T and that with respect to the basis (a, c) the transformation T is represented by an invertable seven-dimensional matrix $T(a, c)$ with integral entries

$$TU = V, \text{with } T(a, c) \in \mathrm{GL}(7, \mathbb{Z}) \simeq \mathrm{Aut}(M) \tag{16}$$

with GL(7, $\mathbb{Z}$) the general linear group of the seven-dimensional invertible integral matrices and Aut(M) the automorphism group of the $\mathbb{Z}$-module M.

For the prismatic forms considered in this work it is always possible to choose the point-group equivalent vertices U and V in such a way that they have the same *planar indices* $n_1, \ldots, n_6$ (axial case) or the same *axial index* n_7 (planar case). Accordingly, the form can be decomposed into the Cartesian product of a two-dimensional heptagrammal form and a one-dimensional vertical edge. The transformations T for these special cases are presented in the next two subsections.

A1.1. Planar heptagrammal forms. The simplest case of a heptagram is the regular heptagon (seven vertices), followed by the star heptagons with Schläfli symbols {7/2} and {7/3} having 14 and 21 vertices, respectively (Coxeter, 1961), as shown in Fig. 8. The next heptagram is a combination of these three and has 42 vertices, as represented in Fig. 9, together with an indication of the corresponding planar indices. Other simple heptagrammal examples can be found in the axial views of the forms given in Figs. 4(*b*), 6 and 7. More complex heptagrams occur in the GroEL–GroES complex when considering folding points at the C^{α} positions of tertiary structures, as discussed in part II. Here, the point groups of a number of simple planar forms are presented.

A1.2. Regular heptagon {7/1}. The point group of the regular heptagon is $K_0 = 7m$, with as generators a rotation R by an angle $\varphi = 2\pi/7$ and a reflection m,

$$K_0 = \langle R, m | R^7 = m^2 = (Rm)^2 = 1 \rangle. \tag{17}$$

On the (a, c) basis these generators are represented by

$$R(a, c) = \begin{pmatrix} 0 & 0 & 0 & 0 & 0 & -1 & 0 \\ 1 & 0 & 0 & 0 & 0 & -1 & 0 \\ 0 & 1 & 0 & 0 & 0 & -1 & 0 \\ 0 & 0 & 1 & 0 & 0 & -1 & 0 \\ 0 & 0 & 0 & 1 & 0 & -1 & 0 \\ 0 & 0 & 0 & 0 & 1 & -1 & 0 \\ 0 & 0 & 0 & 0 & 0 & 0 & 1 \end{pmatrix},$$

$$m(a, c) = \begin{pmatrix} 0 & 0 & 0 & 0 & 0 & 1 & 0 \\ 0 & 0 & 0 & 0 & 1 & 0 & 0 \\ 0 & 0 & 0 & 1 & 0 & 0 & 0 \\ 0 & 0 & 1 & 0 & 0 & 0 & 0 \\ 0 & 1 & 0 & 0 & 0 & 0 & 0 \\ 1 & 0 & 0 & 0 & 0 & 0 & 0 \\ 0 & 0 & 0 & 0 & 0 & 0 & 1 \end{pmatrix}. \tag{18}$$

This point group is also the Euclidean symmetry group of all the (planar) heptagrammal forms considered here.

A1.3. Star heptagon {7/2}. The point group of this form is generated by K_0 and by the planar scaling transformation $S_{-\mu_E}$, which transforms the vertices of the larger heptagon into the corresponding vertices of the central heptagon (see Fig. 8). The radial scaling factor is $-\mu_E = 1 - 2\cos\varphi + 2\cos 2\varphi = -0.6920\ldots$ and the matrix representation is

$$S_{-\mu_E}(a, c) = \begin{pmatrix} 2 & -2 & 1 & 0 & -1 & 2 & 0 \\ 0 & 0 & -1 & 1 & -1 & 1 & 0 \\ 2 & -2 & 1 & -1 & 0 & 1 & 0 \\ 1 & 0 & -1 & 1 & -2 & 2 & 0 \\ 1 & -1 & 1 & -1 & 0 & 0 & 0 \\ 2 & -1 & 0 & 1 & -2 & 2 & 0 \\ 0 & 0 & 0 & 0 & 0 & 0 & 1 \end{pmatrix}. \tag{19}$$

The point group of {7/2} is

$$K_{\{7/2\}} = \langle R, m, S_{-\mu_E} \rangle. \tag{20}$$

This point group is of infinite order. As the number of vertices in {7/2} is finite, $K_{\{7/2\}}$ is not its symmetry group, but only a *structural group* of this heptagram. This concept is defined in Janner (2001*a*). $K_{\{7/2\}}$ is the symmetry group of the infinite set of self-similar star heptagons {7/2}.

A1.4. Star heptagon {7/3}. The point group of this form is

$$K_{\{7/3\}} = \langle R, m, S_{-\mu_C}, S_{\mu_D} \rangle, \tag{21}$$

where

$$S_{-\mu_C}(a, c) = \begin{pmatrix} 1 & 1 & -2 & 0 & 2 & -1 & 0 \\ 0 & 2 & -1 & -2 & 2 & 1 & 0 \\ -1 & 1 & 0 & -1 & 0 & 1 & 0 \\ 1 & 0 & -1 & 0 & 1 & -1 & 0 \\ 1 & 2 & -2 & -1 & 2 & 0 & 0 \\ -1 & 2 & 0 & -2 & 1 & 1 & 0 \\ 0 & 0 & 0 & 0 & 0 & 0 & 1 \end{pmatrix}, \tag{22}$$

$$S_{\mu_D}(a,c)=\begin{pmatrix}-2&1&0&0&0&-1&0\\0&-1&1&0&0&-1&0\\-1&1&-1&1&0&-1&0\\-1&0&1&-1&1&-1&0\\-1&0&0&1&-1&0&0\\-1&0&0&0&1&-2&0\\0&0&0&0&0&0&1\end{pmatrix}, \quad (23)$$

with scaling factors given by

$$-\mu_C=-2\cos\varphi-4\cos 2\varphi=-0.35689\ldots,$$
$$\mu_D=-1+2\cos\varphi=0.24697\ldots. \quad (24)$$

A1.5. Other heptagrammal forms. Indicated here are additional scaling transformations occurring in GroEL or in GroES molecular forms. The subscripts characterize the scaling factors from the heptagon labelled A (or B) to that labelled by the subscript, as already performed in the cases discussed so far. In particular the points at M and at N of Fig. 4(b) are related to B by the scaling transformation S_{μ_N} and its inverse $S_{\lambda_N}=S_{\mu_N}^{-1}$. The point F is scaled from B by $S_{\mu_F}=S_{\mu_E}^2$, whereas H (see Fig. 7) is scaled from A by μ_H and I from B by $\mu_C\mu_E=\mu_D$. In this case

$$S_{\mu_N}(a,c)=\begin{pmatrix}4&-3&2&0&-2&3&0\\0&1&-1&2&-2&1&0\\3&-3&3&-1&0&1&0\\1&0&-1&3&-3&3&0\\1&-2&2&-1&1&0&0\\3&-2&0&2&-3&4&0\\0&0&0&0&0&0&1\end{pmatrix}, \quad (25)$$

$$S_{\mu_H}(a,c)=\begin{pmatrix}1&-1&1&0&-1&1&0\\0&0&0&1&-1&0&0\\1&-1&1&0&0&0&0\\0&0&0&1&-1&1&0\\0&-1&1&0&0&0&0\\1&-1&0&1&-1&1&0\\0&0&0&0&0&0&1\end{pmatrix}, \quad (26)$$

with scaling factors

$$\mu_N=2-4\cos\varphi+2\cos 2\varphi-2\cos 3\varphi=0.862\ldots, \quad (27)$$

$$\mu_H=-1-4\cos\varphi-2\cos 2\varphi-4\cos 3\varphi=0.554\ldots. \quad (28)$$

A1.6. Axial heptagrammal forms. An axial form is an edge of a heptagrammal prismatic form and has two vertices U, V with same planar indices

$$U=(n_1\ \ldots\ n_6,n_7),\quad V=(n_1\ \ldots\ n_6,n_7+k),\quad n_i,k\in\mathbb{Z}. \quad (29)$$

From discussion of the planar forms it follows that the planar indices occurring in the forms of GroEL–GroES are point-group-equivalent to either $(\bar{1}\ \ldots\ \bar{1})$ or $(1\ \ldots\ 1)$, which are the planar indices of vertices labelled A and $B=-A$, respectively. Let us consider the second case. (The first case can be treated in exactly the same way.) There is then a crystallographic scale-rotation T transforming $B(n_7)$ into U; in the (a,c) basis one has

$$T(a,c)(1\ 1\ 1\ 1\ 1\ 1,n_7)=(n_1\ \ldots\ n_6,n_7). \quad (30)$$

Consider the parabolic point-group element P transforming $a_1=(1\,0\ \ldots\ 0,0)$ into $Pa_1=a_1+a_7=(1\,0\ \ldots\ 0,1)$ and leaving the other basis vectors invariant. It has the matrix representation

$$P(a,c)=\begin{pmatrix}1&0&0&0&0&0&0\\0&1&0&0&0&0&0\\0&0&1&0&0&0&0\\0&0&0&1&0&0&0\\0&0&0&0&1&0&0\\0&0&0&0&0&1&0\\1&0&0&0&0&0&1\end{pmatrix}. \quad (31)$$

Then U is transformed to V by a parabolic transformation P_T^k conjugated to P^k, the kth power of P,

$$P_T^kU=V\quad\text{with}\quad P_T^k=TP^kT^{-1}. \quad (32)$$

One then has $P^kB(n_7)=B(n_7+k)$. The parabolic transformation P is the generator of the point group of the axial form. The union of the point groups of the planar and axial forms generates the point group of the given prismatic form. These considerations apply to all three $\mathbb{Z}$-modules M_t, M_c and M_s given in (4), each with its own (a,c) basis, leading to the same matrix representation,

$$P_t(a_t,c_t)=P_c(a_c,c_c)=P_s(a_s,c_s)=P(a,c) \quad (33)$$

with

$$P_c=S_{\lambda_N}^{-1}P_tS_{\lambda_N},\quad P_s^6=S_{\mu_E}P_c^4S_{\mu_E}^{-1}. \quad (34)$$

There is a $\mathbb{Z}$-module and a heptagrammal point group common to all the molecular forms of the GroEL–GroES complex. The existence of a common $\mathbb{Z}$-module follows from the fact that, up to rational factors, the various bases differ by irrational factors μ_E and λ_N which are scaling factors of the heptagrammal transformations S_{μ_E} and S_{λ_N}, respectively. The common point group can be obtained in the same way as above. This is interesting and probably not accidental, but non-essential here, so that further details are omitted.

The careful reading of the first manuscript by B. Souvignier and his pertinent suggestions have greatly helped the author to improve the presentation. Thanks are expressed to R. de Gelder for valuable remarks and to Annalisa Fasolino for stimulating discussions.

References

Boisvert, D. C., Wang, J., Otwinowski, Z., Horwich, A. L. & Sigler, P. B. (1996). *Nature Struct. Biol.* **3**, 170–177.

Braig, K., Otwinowski, Z., Hedge, R., Boisvert, D. C., Joachimiak, A., Horwich, A. L. & Sigler, P. B. (1994). *Nature (London)*, **371**, 578–586.

Branden, C. & Tooze, J. (1999). *Introduction to Protein Structure*, 2nd ed. New York: Garland Publishing.

Bürger, M. J. (1956). *Elementary Crystallography*. New York: John Wiley.

Coxeter, H. S. M. (1961). *Introduction to Geometry*. New York: John Wiley.
Hunt, J. F., Weaver, A. J., Landry, S. J., Gierasch, L. & Deisenhofer, J. (1996). *Nature (London)*, **379**, 37–45.
Janner, A. (2001*a*). *Acta Cryst.* A**57**, 378–388.
Janner, A. (2001*b*). *Cryst. Eng.* **4**, 119–129.
Janner, A. (2002*a*). *Struct. Chem.* **13**, 279–289.
Janner, A. (2002*b*). *Z. Kristallogr.* **217**, 408–414.
Janner, A. (2002*c*). *Acta Cryst.* A**58**, 334–345.
Janner, A. (2003*a*). *Acta Cryst.* D**59**, 795–808.
Janner, A. (2003*b*). *Proteins*, **51**, 126–136.
Lorimer, G. (1997). *Nature (London)*, **388**, 720–723.
Rye, H. S., Burston, S. G., Fenton, W. A., Beechem, J. M., Xu, Z., Sigler, P. B. & Horwich, A. L. (1997). *Nature (London)*, **388**, 792–798.
Saibil, H. & Wood, S. (1993). *Curr. Opin. Struct. Biol.* **3**, 207–213.
Xu, Z., Horwich, A. L. & Sigler, P. B. (1997). *Nature (London)*, **388**, 741–750.